

Cite this article as: Zhang Chun, Qi Chao, Yan Leilei, et al. 3D Effect of Sandwich Panels with Aluminum-Foam-Filled Corrugated Plates Under Out-of-Plane Compression[J]. Rare Metal Materials and Engineering, 2022, 51(01): 36-43.

ARTICLE

# 3D Effect of Sandwich Panels with Aluminum-Foam-Filled Corrugated Plates Under Out-of-Plane Compression

Zhang Chun<sup>1</sup>, Qi Chao<sup>1,2</sup>, Yan Leilei<sup>1</sup>, Zhao Yuliang<sup>3</sup>, Zhang Yunwei<sup>4</sup>

<sup>1</sup> School of Aeronautics, Northwestern Polytechnical University, Xi'an 710072, China; <sup>2</sup> State-Owned Sida Machinery Manufacturing Company, Xianyang 712201, China; <sup>3</sup> School of Mechanical Engineering, Dongguan University of Technology, Dongguan 523808, China; <sup>4</sup> Aeronautics Engineering College, Air Force Engineering University, Xi'an 710051, China

**Abstract:** The out-of-plane compressive behavior of the closed-cell aluminum foam plate, 3 types of empty corrugated plates, and the sandwich panels with 3 types of closed-cell-aluminum-foam-filled corrugated aluminum plates bonded by epoxy resin was investigated. The results show that the aluminum-foam-filled corrugated plates can increase the compressive strength and energy absorption capacity significantly, and obtain more stable mechanical properties. Aluminum-foam-filled corrugated plates have an obvious three-dimensional effect in compression. The smaller the strength of sandwich panel, the more obvious the three-dimensional extension deformation. The aluminum-foam-filled corrugated plates made of different aluminum alloy plates with different strengths all show similar mechanical properties. The 3003 aluminum alloy plate with good formability, high corrosion resistance, and good weldability is suitable for face plates and corrugated plates.

**Key words:** aluminum foam; corrugated plate; buckling; interaction effect; 3D effect

Due to the high strength, high stiffness, excellent energy absorption, and good blast resistance, the composite sandwich panels composed of two face plates and one core material are widely used for modern engineering fields, such as the aerospace, aircraft, automotive, and buildings, as attractive load carrying constructions<sup>[1-4]</sup>. A great deal of core configurations and filled materials were proposed in last several decades. Corrugated and periodic lattice cores (pyramid, tetrahedron, and Kagome configurations) and porous-foam/honeycomb sandwich panels are generally preferred structures, especially in the multifunctional application<sup>[5-9]</sup>. Under the out-of-plane compressive loading or three-point bending loading, these panels usually suffer a peak stress at a rather low strain and then become soft rapidly due to core buckling and/or node failure. To avoid these phenomena, several studies showed that the hybrid corrugated composite/core (metal foam, polymer foam, balsa, and concrete) sandwich structures can effectively enhance the performance (peak compressive strength and energy

absorption ability) with fixed total mass<sup>[2,9-12]</sup>. Therefore, the preparation of foam sandwich structure and the corresponding mechanical properties were investigated<sup>[13-15]</sup>.

The node or joint produced by laser welding method or interlocking technique<sup>[2,9,16]</sup> requires expensive laser equipment, finishing equipment, and welding equipment. The complex manufacturing method seriously restricts the manufacturing efficiency and use scale of high cost. Thus, this research presents a convenient preparation method for sandwich panel. The sandwich panels consisting of corrugated plates filled with aluminum foam were prepared using epoxy resin for bonding. The bonding order is as follows: the upper face plate, aluminum foam, corrugated plate, aluminum foam, and lower face plate (Fig.1). The purpose of this research is to study the deformation characteristics of the sandwich panel and reveal the enhancement mechanism for mechanical properties and energy adsorption capacity of the sandwich panel. In addition, the buckling mode of corrugated plates has been widely investigated, while the in-plane deformation of

Received date: January 18, 2021

Foundation item: Shaanxi Natural Science Basic Research Project (2020JQ-114, 2020JQ-113); National Natural Science Foundation of China (11702326); Chinese Postdoctoral Science Foundation (2018M633493)

Corresponding author: Yan Leilei, Ph. D., Associate Professor, School of Aeronautics, Northwestern Polytechnical University, Xi'an 710072, P. R. China, Tel: 0086-29-88460479, E-mail: yanleilei@nwpu.edu.cn

Copyright © 2022, Northwest Institute for Nonferrous Metal Research. Published by Science Press. All rights reserved.

corrugated plates is seldom studied. This research investigated both the buckling modes and in-plane deformation of corrugated plates. It is of great significance to deeply understand the deformation morphology and mechanism of aluminum-foam-filled corrugated plates of sandwich panels.

## 1 Experiment

Three kinds of aluminum alloy plates were selected: 2024 aluminum alloy (density  $\rho_s=2.85 \text{ g/cm}^3$ ; conditional yield strength  $\sigma_{0.2}=250 \text{ MPa}$ ), 3003 aluminum alloy (density  $\rho_s=2.75 \text{ g/cm}^3$ ; conditional yield strength  $\sigma_{0.2}=120 \text{ MPa}$ ), and 7075 aluminum alloy (density  $\rho_s=2.82 \text{ g/cm}^3$ ; conditional yield strength  $\sigma_{0.2}=455 \text{ MPa}$ ). Some of the plates were deformed into corrugated configuration, and others remained the plate state. These aluminum alloys were cut into a predetermined size by electro-discharge machining (EDM). Closed-cell aluminum foam was used in this research. The average pore size of aluminum foam is 4 mm, the density is  $630.00 \text{ kg/m}^3$ , and the corresponding porosity is about 77.5%. Triangular prisms of aluminum foam were cut to precisely fit the void space of the corrugated plates by EDM from the aluminum foam sheet as the filling material.

The preparation procedure for sandwich panels with closed-cell-aluminum-foam-filled corrugated plates is shown in Fig. 1. Both the face plates and corrugated plates of the sandwich panels were made of the same aluminum alloy plates. All the components were bonded by epoxy resin for 24 h. Meanwhile, the empty corrugated plates and the cubic closed-cell aluminum foam specimens with the size of  $40 \text{ mm} \times 40 \text{ mm} \times 80 \text{ mm}$  were also prepared for comparison.

As shown in Fig. 2, the length, width, and height of empty/filled specimens were 108, 20, and 19.2 mm, respectively. The compression direction was set as Z axis. The length, width, and height of closed-cell aluminum foam specimens were 40, 40, and 80 mm, respectively. The height direction was the compression direction. According to the used material and filling status, the specimens were named as aluminum foam, 2024-empty, 3003-empty, 7075-empty, 2024-filled, 3003-filled, and 7075-filled, and their fundamental physical parameters are displayed in Table 1.

The quasi-static out-of-plane compression tests were conducted by the hydraulic testing machine (INSTRON 8803)

at room temperature. The compression rate was 4.2 and 1.0 mm/min for empty specimens and foam-filled specimens, respectively. Correspondingly, the nominal strain rate was  $8.7 \times 10^{-4} \text{ s}^{-1}$  for all the specimens. In order to ensure that the densification stage was achieved during compression, the nominal strain at the end of the test was set as at least 50%. Images were collected by camera every 10 s during the compression process.

Due to the sandwich structure of corrugated plates and aluminum foam, the deformation includes not only buckling deformation but also the in-plane deformation. The buckling deformation was recorded in real time by camera. In order to obtain the in-plane deformation of corrugated plates, the camera and Artec Space Spider (Artec 3D) were used.

## 2 Results

Fig. 3 shows the compressive stress-strain curve of closed-cell aluminum foam at the strain rate of  $8.7 \times 10^{-4} \text{ s}^{-1}$ . The insets of points A~E show the appearances of aluminum specimens at different strains of 0%, 5%, 10%, 30%, and 50%, respectively. As shown in Fig. 3, the compressive stress reaches a maximum value, then drops slightly, and changes to a plateau. After the strain reaches to 28%, there is an obvious decrease in the stress plateau, because the aluminum foam has obvious crushing and slagging phenomena, resulting in the reduction in effective area and stress (inset of point D). Finally, the compressive stress-strain curve rises sharply, indicating that the aluminum foam is densified. The compression behavior of the researched aluminum foam has three typical regions, namely linear region, plateau region, and densification region, which are similar to that of other foam materials<sup>[17-20]</sup>.

In addition, the compressive stress-strain curves of corrugated plates using different kinds of aluminum alloys are shown in Fig. 4. As shown in Fig. 4a, there is an obvious compressive stress drop, indicating that the slippage and debonding occur at the bonding points. Fig. 5 shows the deformation appearances of 3003-empty specimens under different strains and A~I correspond to the points A~I in Fig. 4a and 4b, respectively. The rise of the stress-strain curve from point C to point D is due to the starting buckling of the corrugated plate. The rise of the stress-strain curve from point F to point H is because buckling deformation is initiated again.

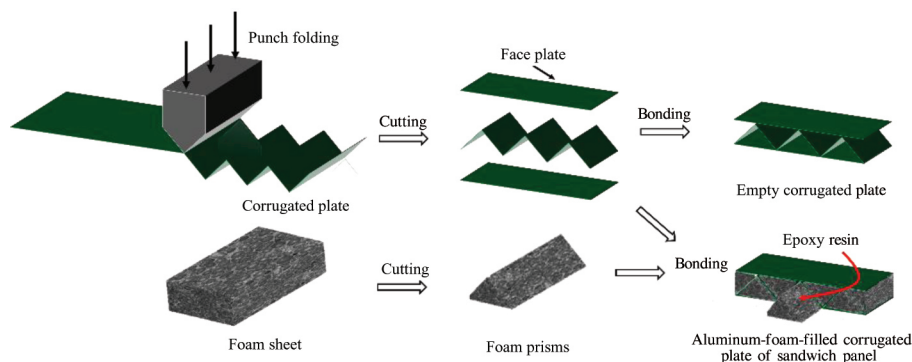


Fig. 1 Schematic diagram of preparation process for empty corrugated plate and aluminum-foam-filled corrugated plate of sandwich panels

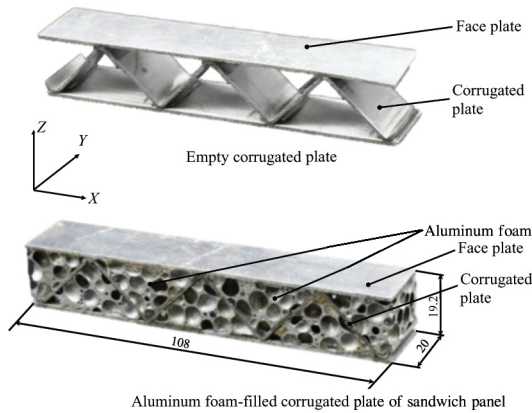


Fig.2 Appearances of empty corrugated plate (a) and aluminum-foam-filled corrugated plate (b)

Table 1 Fundamental physical parameters of different specimens

Specimen	Mass, $m/g$	Volume, $V/\times 10^{-5} m^3$	Density, $\rho_c/kg \cdot m^{-3}$	Relative density, $\rho_r$
Aluminum foam	80.64	12.8	630.00	0.080
2024-empty	8.35		224.75	0.028
3003-empty	7.82		210.49	0.027
7075-empty	8.40	3.72	226.10	0.029
2024-filled	35.56		957.15	0.121
3003-filled	34.37		925.12	0.117
7075-filled	36.02		969.53	0.123

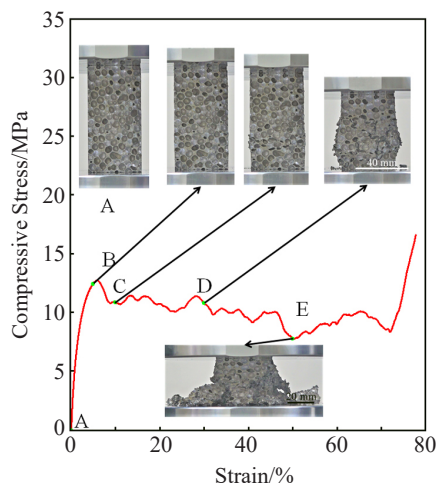


Fig.3 Compressive stress-strain curve of closed-cell aluminum foam at strain rate of  $8.7 \times 10^{-4} s^{-1}$

As for the corrugated plates made of 2024 alloy, the stress is decreased continuously after the peak stress, because there is only debonding failure mode in the whole failure process. If no first and secondary buckling phenomena occur, there will be no load increase or second peak stress (Fig.4c).

In order to investigate the difference in mechanical properties of 2024-empty, 3003-empty, and 7075-empty

specimens, the energy absorption capacity per unit volume  $W_v$  is obtained and can be expressed as follows<sup>[2,18]</sup>:

$$W_v = \int_0^{\bar{\varepsilon}} \sigma d\varepsilon \quad (1)$$

where  $\sigma$  is the compressive stress,  $\varepsilon$  is the compression of strain,  $\bar{\varepsilon}$  is defined as 0.5 (when the strain is greater than 0.5, the specimen is densified). Hence, the value of energy absorption capacity per unit volume  $W_v$  can be calculated by the area under the compression stress-strain curve.

Based on Eq. (1), the energy absorption capacity per unit volume  $W_v$  of 2024-empty, 3003-empty, and 7075-empty specimens is  $0.23 \times 10^3$ ,  $0.35 \times 10^3$ ,  $0.41 \times 10^3$  kJ/m<sup>3</sup>, respectively, as listed in Table 2. The 7075-empty specimen with the highest strength has the greatest energy absorption capacity. However, the failure model of 2024-empty corrugated plate only involves the node debonding (Fig. 4c). Thus, its energy absorption capacity is the lowest among these specimens.

Fig.6a shows the compressive stress-strain curves of 2024-filled, 3003-filled, and 7075-filled specimens at the strain rate of  $8.7 \times 10^{-4} s^{-1}$ . Compared with the corrugated plates without the filler of aluminum foam, the compressive stress-strain curves of filled specimens are decreased slightly into a long stress plateau region after the compressive stress reaches the maximum value, but there is no obvious sharp peak. In the compression process, the failure of aluminum foam happens almost simultaneously with the buckling of corrugated plates, as shown in Fig. 7. With further increasing the strain, although the aluminum foam is damaged, it still acts as a deformation constraint for the corrugated plate, leading to the inconsistent multi-buckling of corrugated plates due to the particularity of aluminum foam, i. e., different bonding capacities of corrugated plates. However, the greater the buckling, the greater the critical load and the higher the stress.

The energy absorption capacity per unit volume of aluminum-foam-filled corrugated plates calculated by Eq. (1) is  $13.49 \times 10^3$ ,  $13.37 \times 10^3$ , and  $15.60 \times 10^3$  kJ/m<sup>3</sup> for 2024-filled, 3003-filled, and 7075-filled specimens, respectively, as shown in Fig.6b and Table 2. Although there are great differences in mechanical properties of these three aluminum alloys, the difference in energy absorption capacity of aluminum-foam-filled corrugated plates is very small, only 14.3%.

### 3 Discussion

#### 3.1 Interaction effect

The compressive stress-strain curves of aluminum foam, 3003-empty, and 3003-filled specimens are shown in Fig.8. In addition, the algebraic sum of compressive stress of aluminum foam and 3003-empty specimen is also presented in Fig.8, as indicated by the red line of “foam+empty”.

Fig. 8 shows that the compressive stress of 3003-filled specimen is almost twice as much as the compressive stress of “foam+empty” before the strain reaches 30%. After strain reaches 30%, the rapid rise of compressive stress-strain curve of 3003-filled specimen indicates that the 3003-filled specimen enters the densification region earlier than the aluminum foam and 3003-empty specimens. The strains

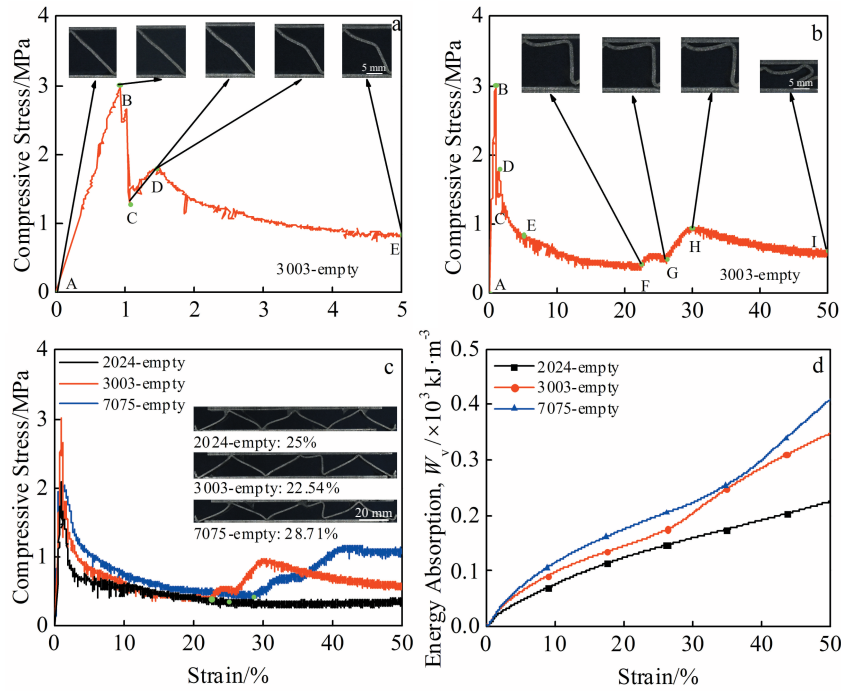


Fig.4 Compressive stress-strain curves of 3003-empty specimens at strain of 0%~5% (a) and 0%~50% (b); compressive stress-strain curves (c) and energy absorption capacity per unit volume (d) of 2024-empty, 3003-empty, and 7075-empty specimens (insets are appearance of specimens at different strains)

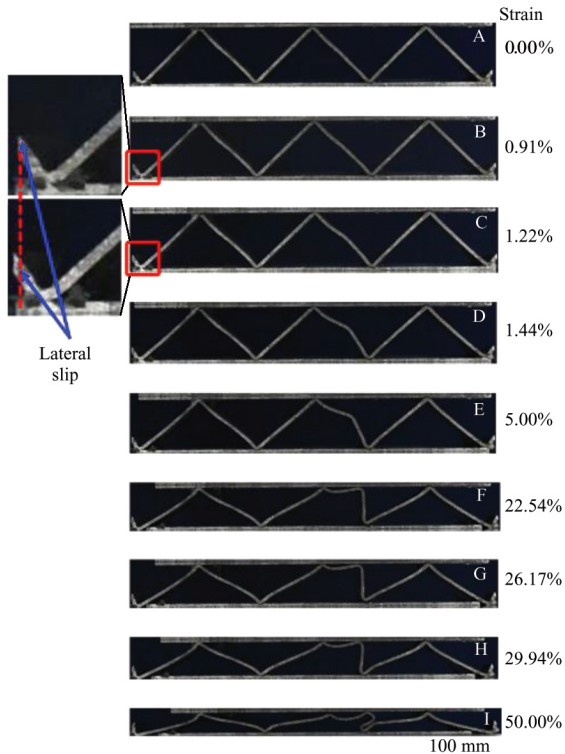


Fig.5 Deformation appearances of 3003-empty specimens under compression stress at strain of 0.00%~50.00% (A~I represent the points A~I in Fig.4a and 4b)

corresponding to the densification region of aluminum foam and 3003-empty are both beyond 50%.

The failure mode of aluminum foam is crushing and dropping (Fig. 3). As for the corrugated plates without aluminum foam, the main damage characteristic is debonding at the bonding points (Fig. 5). As for the aluminum-foam-filled corrugated plates, the damage characteristic changes. Aluminum foam is hard to crush due its characteristic and the bonding points are firm because of the support of aluminum foam which can enhance the buckling, thereby greatly improving the critical force. These factors result in better interaction effect for aluminum-foam-filled corrugated plates.

It is noted that the influence of different aluminum alloys on the compressive properties of aluminum-foam-filled corrugated plates is slight, as shown in Fig. 6. The 3003 aluminum alloy is optimal because of its good formability, high corrosion resistance, good weldability, and low cost.

In addition, compared with the sandwich panels without aluminum foam, the sandwich panels filled with closed aluminum foam and bonded by epoxy resin have more stable mechanical properties. As shown in Fig. 6, the compressive stress-strain curve of 3003-empty and 7075-empty specimens has the second peak, whereas that of 2024-specimen does not. The compressive stress-strain curves of different sandwich panels filled with closed-aluminum-foam are similar, indicating that after reaching the peak stress value, the specimens are densified and then the stress starts to rise again.

### 3.2 Specific energy absorption

The peak compressive strength and energy absorption are the parameters to represent the mechanical properties. The specific peak compressive strength  $\sigma_p/\rho_c$  and specific energy

**Table 2 Mechanical properties of different specimens**

Specimen	Peak stress, $\sigma_p$ /MPa	Relative compressive strength, $\sigma_p/\rho_f\sigma_Y$	Peak strain, $\varepsilon_p$ /%	Elastic modulus, $E$ /MPa	Energy absorption per unit volume, $W_v/\times 10^3 \text{ kJ}\cdot\text{m}^{-3}$	Energy absorption per unit mass, $W_m/\text{kJ}\cdot\text{kg}^{-1}$	Relative specific energy absorption, $W_m\rho_s/\sigma_Y\varepsilon$
Aluminum foam	12.75	0.761	5.82	735.50±5.88	5.15	8.17	0.62
2024-empty	2.08	0.348	0.92	251.27±2.80	0.23	1.02	0.08
3003-empty	3.01	0.538	0.91	338.13±4.26	0.35	1.66	0.13
7075-empty	2.30	0.383	0.58	437.43±1.24	0.41	1.81	0.14
2024-filled	22.60	0.888	9.14	659.03±3.02	13.49	14.09	1.06
3003-filled	21.94	0.892	8.56	662.33±5.74	13.37	14.45	1.09
7075-filled	23.44	0.910	8.19	635.62±2.29	15.60	16.09	1.21

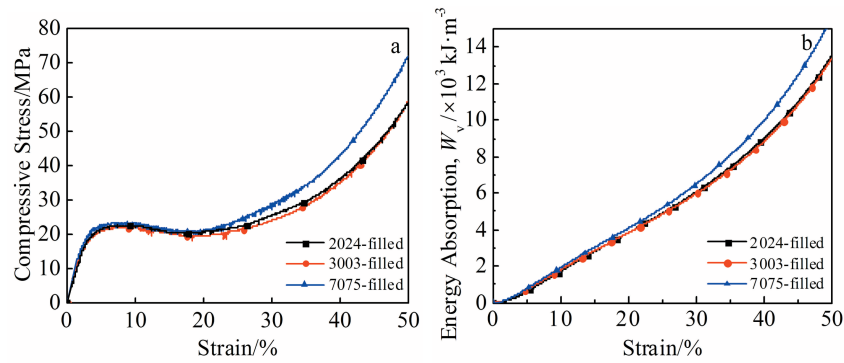


Fig.6 Compressive stress-strain curves (a) and energy absorption per unit volume (b) of 2024-filled, 3003-filled, and 7075-filled specimens at strain rate of  $8.7 \times 10^{-4} \text{ s}^{-1}$

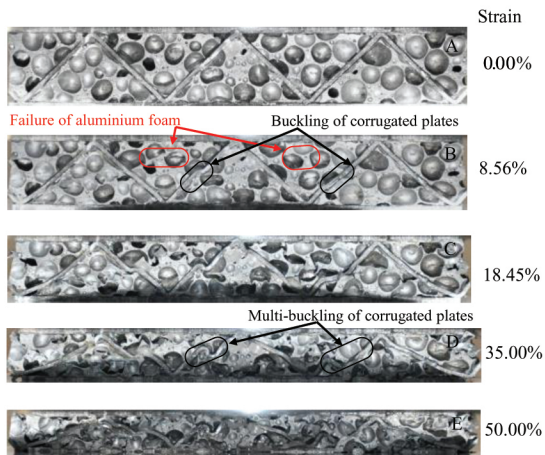


Fig.7 Deformation appearances of 3003-filled specimens under compression stress at strain of 0.00%~50.00%

absorption (SEA)  $W_m/\rho_c$  are proposed.  $\rho_c$  is the density of the panel, which can be calculated by Eq.(2), as follows:

$$\rho_c = \rho_{Al}v_{Al} + \rho_f(1 - v_{Al}) \quad (2)$$

where  $\rho_{Al}$  and  $\rho_f$  denote the density of aluminum alloy and foam, respectively;  $v_{Al}$  is the volume proportion of the corrugated aluminum alloy plate. The  $\rho_f$  can be obtained by the definition of the density, i.e.,  $\rho_f$  equals to the mass divided by the volume.

In order to compare the quasi-static out-of-plane compressive properties of sandwich panels with different plates, such as empty corrugated plates, foam-filled corrugated plates, diamond plates, square-honeycomb plates, and pyramidal truss plates, the relative specific peak compressive strength and relative SEA are normalized using the properties of 304 stainless steel.

The relative specific peak compressive strength can be obtained by  $(\sigma_p/\rho_c)/(\sigma_Y/\rho_s)$ , i.e.,  $\sigma_p/\rho\sigma_Y$ , where  $\sigma_Y$  and  $\rho_s$  are the yield stress and density of 304 stainless steel, respectively.  $\rho = \rho_f/\rho_s$  is the relative average density of sandwich panels.

SEA is an important mass-related parameter, which can be defined as the energy absorption per unit mass  $W_m$ <sup>[18-22]</sup>, as follows:

$$W_m = \frac{W_v}{\rho_c} \quad (3)$$

The relative SEA can be calculated by  $W_m/(W_s/\rho_s)$  with  $W_s = \sigma_Y\varepsilon$ , i.e.,  $SEA = W_m\rho_s/\sigma_Y\varepsilon$ .

The relative peak compressive strength and relative SEA of sandwich panels with different corrugated plates are shown in Fig.9. Although the relative peak compressive strength of the aluminum-foam-filled corrugated plates is ordinary, the relative SEA is obviously better than that of the corrugated plates without aluminum foam, the diamond and pyramidal truss panels, or the square-honeycomb panels. This phenomenon reflects that the aluminum-foam-filled corrugated plates

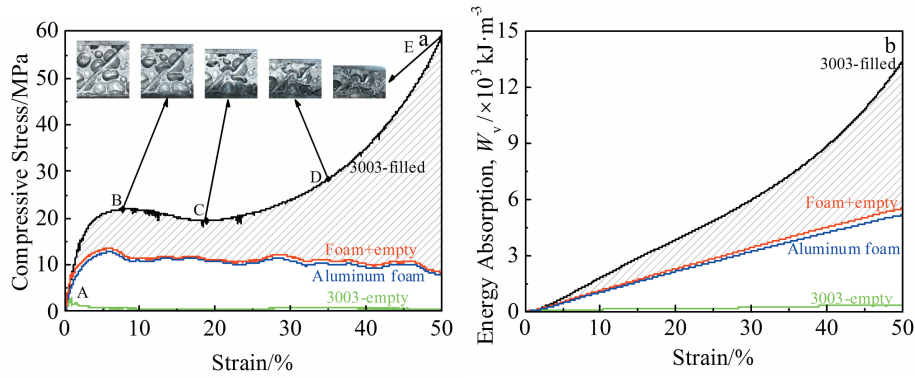


Fig.8 Compressive stress-strain curves (a) and energy absorption per unit volume (b) of different specimens at strain rate of  $8.7 \times 10^{-4} \text{ s}^{-1}$

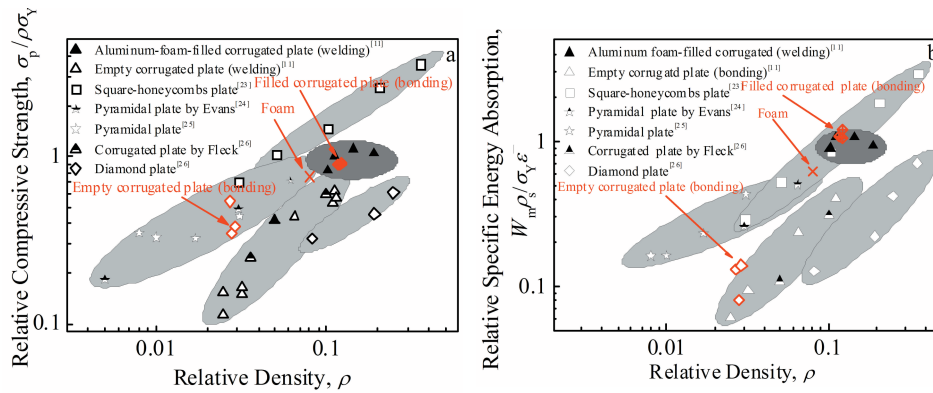


Fig.9 Relative peak compressive strength (a) and relative specific energy absorption (b) of sandwich panels with different corrugated plates

have high compressive strength and are stable under high stress, which improves the energy absorption and hinders the sudden break.

### 3.3 Three-dimensional effect

The 2024-filled, 3003-filled, and 7075-filled specimens were compressed under the strain of 70% which corresponds to the deformation of 13.4 mm.

Because there is no restriction in the other two directions, the reduction in specimen size along compression direction causes the increase in size along other directions, namely the Poisson effect. However, different materials of the surface plates and corrugated plates will lead to different degrees of increase. Actually, the specimens were severely damaged after the tests.

The deformed surface plates of sandwich panels made of 2024 Al alloys, 3003 Al alloys, and 7075 Al alloys are shown

in Fig. 10a~10c, respectively; while the deformed corrugated plates made of 2024 Al alloys, 3003 Al alloys, and 7075 Al alloys are shown in Fig. 10d~10f, respectively. The width is 23.3, 23.9, and 23.1 mm for surface plates of 2024 Al alloys, 3003 Al alloys, and 7075 Al alloys, respectively. The width is 26.8, 27.4, and 26.4 mm for corrugated plates of 2024 Al alloys, 3003 Al alloys, and 7075 Al alloys, respectively. It is obvious that the dimension along the width direction is increased, compared with the original length of 20 mm. Meanwhile, the three-dimensional effect is clearly revealed by Fig. 11 which shows the deformed corrugated plates of 2024 Al alloys, 3003 Al alloys, and 7075 Al alloys by Artec Space Spider software. The strength of corrugated plates of 2024 Al alloy, 3003 Al alloy, and 7075 Al alloy is 250, 120, and 455 MPa, respectively. The greater the strength, the more difficult the deformation and the less obvious the three-dimensional

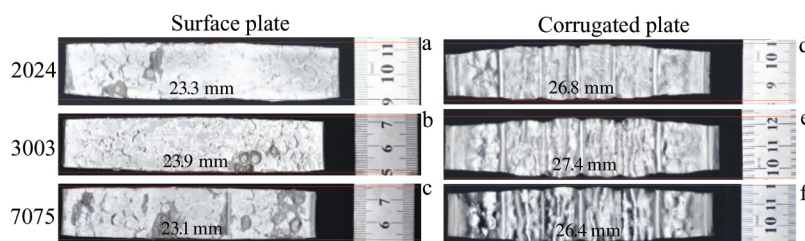


Fig.10 Deformed surface plates (a-c) and corrugated plates (d-f) of 2024 Al alloys (a, d), 3003 Al alloys (b, e), and 7075 Al alloys (c, f)

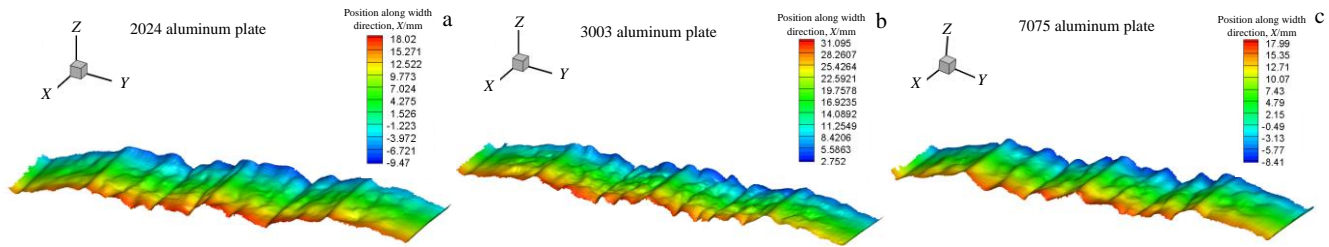


Fig.11 Simulated deformed corrugated plates of 2024 Al alloys (a), 3003 Al alloys (b), and 7075 Al alloys (c)

effect. Hence, the width of surface plates of 2024 Al alloys, 3003 Al alloys, and 7075 Al alloys is increased by 16.5%, 19.5%, and 15.5%, respectively; the width of corrugated plated is increased by 34.0%, 37.0%, and 32.0%, respectively. This result is positively associated with hardness range. Besides, the width increment of surface plates is smaller than that of corrugated plates, because just one side of surface plates is influenced by friction from the increase of aluminum foam owing to Poisson effect, while both the upper and lower sides of corrugated plates are affected by friction.

Therefore, the three-dimensional effect is obvious. With increasing the width, the three-dimensional effect may be weakened, which should be further studied. The aluminum-foam-filled corrugated 3003 aluminum alloy plate is optimal because the 3003 aluminum alloy has good formability, high corrosion resistance, and good weldability.

#### 4 Conclusions

1) The closed-aluminum-foam-filled corrugated plates can increase the compressive strength and energy absorption capacity significantly. The sandwich panels filled with closed foam and bonded by epoxy resin have more stable mechanical properties.

2) Aluminum-foam-filled corrugated plates have an obvious three-dimensional effect under compression. The smaller the strength of aluminum alloy panel, the more obvious the three-dimensional extension deformation.

3) The aluminum-foam-filled corrugated plates made of three different aluminum alloys with different strengths have similar mechanical properties. In general, 3003 aluminum alloy plates with good formability, high corrosion resistance, and good weldability are optimal as face plates and corrugated plates.

#### References

- Wadley H N G, Fleck N A, Evans A G. *Composites Science and Technology*[J], 2003, 63(16): 2331
- Yan L L, Yu B, Han B et al. *Composites Science and Technology* [J], 2013, 86: 143
- Cheng Yuansheng, Liu Manxia, Zhang Pan et al. *International Journal of Mechanical Sciences*[J], 2018, 145: 378
- Yazici M, Wright J, Bertin D et al. *Composite Structures*[J], 2014, 110: 98
- Kazemahvazi S, Zenkert D. *Composites Science and Technology* [J], 2009, 69(7): 913
- Kazemahvazi S, Tanner D, Zenkert D. *Composites Science and Technology*[J], 2009, 69(7): 920
- Fan H L, Fang D N, Chen L M et al. *Composites Science and Technology*[J], 2009, 69(15): 2695
- Xiong J, Ma L, Wu L Z et al. *Composite Structures*[J], 2010, 92(11): 2695
- Yan L L, Jiang W, Zhang C et al. *Polymers*[J], 2019, 11(2): 372
- Sayahlatifi S, Rahimi G H, Bokaei A. *Engineering Structures*[J], 2020, 210: 110 361
- Yan L L, Han B, Yu B et al. *Materials & Design*[J], 2014, 60: 510
- Wang Y M, Shao Y B, Chen C et al. *Thin-Walled Structures*[J], 2020, 148: 106 592
- Hao Qingxian, Qiu Sawei, Hu Yuebo. *Rare Metal Materials and Engineering*[J], 2015, 44(3): 548 (in Chinese)
- Pandey A, Muchhala D, Kumar R et al. *Composites Part B: Engineering*[J], 2020, 183: 107 729
- Zu Guoyin, Sun Xi, Huang Peng et al. *Rare Metal Materials and Engineering*[J], 2017, 46(10): 3141 (in Chinese)
- Wei Kai, Yang Qidong, Ling Bin et al. *Extreme Mechanics Letters*[J], 2018, 23: 41
- Movahedi N, Linul E. *Materials Letters*[J], 2017, 206: 182
- Yan Leilei, Zhao Xue, Zhao Jingbo et al. *Rare Metal Materials and Engineering*[J], 2018, 47(2): 503 (in Chinese)
- Zhao Xue, Yan Leilei, Lu Tianjian et al. *Journal of Air Force Engineering University (Natural Science Edition)*[J], 2018, 47(2): 503 (in Chinese)
- Zhang Wanbo, Yan Leilei, Zhao Xue et al. *Rare Metal Materials and Engineering*[J], 2019, 48(12): 3911 (in Chinese)
- Liu Qiang, Shen Hao, Wu Yinghan et al. *Composite Structures* [J], 2018, 194: 87
- Cote F, Deshpande V S, Fleck N A et al. *International Journal of Solids and Structures*[J], 2006, 43(20): 6220
- Cote F, Deshpande V S, Fleck N A et al. *Materials Science and Engineering A*[J], 2004, 380(1): 272
- Zok F W, Waltner S A, Wei Z et al. *International Journal of Solids and Structures*[J], 2004, 41(22): 6249
- Zhang Qiancheng, Han Yunjie, Chen Changqing et al. *Science in China Series E: Technological Sciences*[J], 2009, 52(8): 2147
- Chen W G, Wierzbicki T. *Thin-Walled Structures*[J], 2001, 39(4): 287

## 泡沫铝填充波纹夹芯板面外压缩的三维效应

张 纯<sup>1</sup>, 祁 超<sup>1,2</sup>, 闫雷雷<sup>1</sup>, 赵愈亮<sup>3</sup>, 张耘伟<sup>4</sup>

(1. 西北工业大学 航空学院, 陕西 西安 710072)

(2. 国营四达机械制造公司, 陕西 咸阳 712201)

(3. 东莞理工学院 机械工程学院, 广东 东莞 523808)

(4. 空军工程大学 航空工程学院, 陕西 西安 710051)

**摘 要:** 研究了闭孔泡沫铝板、3种空心波纹铝板和3种用环氧树脂粘接而成的闭孔泡沫铝填充波纹铝板的平面外压缩性能。泡沫填充波纹铝板不仅能显著提高抗压强度和吸能能力, 而且力学性能更加稳定。泡沫填充波纹板具有明显的三维压缩效果。铝合金板材强度越小, 三维延伸变形越明显。由3种不同强度的铝合金板制成的泡沫铝填充波纹板具有相似的力学性能。成形性好、耐腐蚀性高、可焊性好的3003铝合金板非常适合作为面板和波纹板。

**关键词:** 泡沫铝; 波纹板; 屈曲; 耦合效应; 三维效应

---

作者简介: 张 纯, 男, 1988年生, 博士, 西北工业大学航空学院, 陕西 西安 710072, 电话: 029-88460479, E-mail: c.zhang@nwpu.edu.cn